Strain-induced local distortions and orbital ordering in $Nd_{0.5}Sr_{0.5}MnO_3$ manganite films

Q. Qian,[1] T. A. Tyson,[1] C.-C. Kao,[2] W. Prellier,[3] J. Bai,[4] A. Biswas,[3] and R. L. Greene[3]

[1]*Department of Physics, New Jersey Institute of Technology, Newark, New Jersey 07102*
[2]*Brookhaven National Laboratory, Upton, New York 11973*
[3]*Center for Superconductivity Research, University of Maryland, College Park, Maryland 20742*
[4]*Oak Ridge National Laboratory, Oak Ridge, Tennessee 37831*

We have performed a detailed study of the long-range and local structure of $Nd_{0.5}Sr_{0.5}MnO_3$ films of varying thicknesses. The detailed nature of the in-plane and out-of-plane d spacings as a function of film thickness was determined. Comparisons between the local structure about Mn and the long-range structure were made. We found that Mn coordination asymmetry exists in thin films and that it is related to orbital ordering. The results yield a confirmation of models of manganite systems, which suggests that biaxial strain enhances electron localization.

Colossal magnetoresistance (CMR) perovskite manganites have attracted a great deal of attention recently because of the interest in understanding the wide range of magnetic and transport properties exhibited by them, and the potential applications of these properties.[1] It is now evident that the properties and the complex phase diagrams of CMR manganites are driven by the close interplay between the charge, spin, and orbital degrees of freedom in the system, although the details of the coupling and the consequences of them are still an active area of research. It is also clear that lattice strain plays an important role in the properties of these materials, which opens up the possibility of optimizing the properties of CMR oxides for specific applications by growing thin CMR films on substrates with different lattice spacing.[2,3]

The first systematic experimental study of the effect of the thickness dependence on the magnetotransport properties of thin films was performed by Jin *et al.*,[2] which was later followed by others.[3,4] The characteristic feature found is that the metal-insulator transition is suppressed in very thin films. Systematic magnetic studies have also been performed.[5–9] O'Donnel *et al.*[9] suggested that the magnetic anisotropy in films seen in many experiments is dominated by strain-induced anisotropy leading to the easy axis, which occurs parallel to or normal to the film plane depending on substrate-induced compression or tension.

The first attempt at quantifying the role of strain in these materials was made by Millis *et al.*[10] who showed that T_c is extremely sensitive to biaxial strain and that T_c reduction is quadratic in the Jahn-Teller (JT) distortion.[11] Recently, a calculation of the phase diagram of tetragonal manganites[12] showed that magnetic degrees of freedom can be indirectly controlled by lattice distortion via orbital degrees of freedom. Specifically, the author argued that by changing the c/a ratio the e_g orbital extending along the elongated Mn-O bond is preferentially occupied.

In addition to the strain-induced changes in transport found in the CMR region ($x \sim 0.3$), interesting and intriguing results were found in the charge-ordered region. Prellier *et al.*[13] found that in $Nd_{0.5}Sr_{0.5}MnO_3$, a metallic state is induced in thick films while thin films remain insulating—with no metal-insulator transition at ~ 150 K as in bulk.[14]

In order to understand the correlation between strain, magnetotransport properties, and orbital ordering in these materials, a detailed characterization of both the long and short-range structure of strained films of varying thicknesses is required. In this paper we present a combined measurement of the local and long-range structure in $Nd_{0.5}Sr_{0.5}MnO_3$ films of varying thicknesses. Most significantly, we find that films with large in-plane strain also exhibit large local Jahn-Teller distortions that might help to explain the charge-order-like behavior of these very thin $Nd_{0.5}Sr_{0.5}MnO_3$ films (as well as films in the CMR region) observed over a broad temperature range.

Films of $Nd_{0.5}Sr_{0.5}MnO_3$ were grown *in situ* using the pulsed laser deposition technique.[15] Substrates used were $LaAlO_3$ (100) (pseudocubic with $a = 3.79$ Å). Sample preparation is described in Ref. 13. Laboratory x-ray-diffraction (XRD) studies showed that the films were (202) oriented. Rutherford backscattering measurements confirmed that the films had the same composition as bulk materials. Mn K_β emission measurements[16] were also performed on the films and revealed that no change in the valence occurred as a function of film thickness. The synchrotron XRD experiments described below were performed on the Oak Ridge National Laboratory's x-ray beamline X14A at the National Synchrotron Light Source (NSLS) at the Brookhaven National Laboratory (BNL). The x-ray energy was set to 8.0468 keV ($\lambda = 1.5406$ Å). The measured diffraction peaks were fit by Gaussian functions and the results are given in Table I. Linearly polarized Mn K-edge absorption spectra in fluorescence mode were measured on the NSLS beamline X21A at the BNL. Measurements were made for films in two orientations: one with the beam E vector nearly perpendicular (E vector $\sim 10°$ from the surface normal) to the surface and one with the E vector in the plane of the film. The near-edge spectra were area normalized.

In Fig. 1, we show the diffraction profiles for two in-plane orthogonal reflections: (3 1 −2) and (1 −5 0) corresponding approximately to the two in-plane Mn-O bond directions.[14] (Note that all reflections are indexed using the unit-cell conventions of Ref. 14.) These measurements correspond to 79° rotations relative to the (202) sample normal. Below, we call these reflections in plane. For the 500-Å films (dashed line) a

TABLE I. $Nd_{0.5}Sr_{0.5}MnO_3$ XRD results; index constants $[h, k, l]$, 2θ diffraction angles, and d spacing determined from synchrotron XRD. ϵ_{hkl} is the effective strain defined in the text.

Index	2θ (deg)	2000 Å d (Å)	$\epsilon_{hkl(\%)}$	2θ (deg)	500 Å d (Å)	$\epsilon_{hkl(\%)}$	Bulk (297 K)[a] d (Å)	Bulk (10 K)[a] d (Å)
2 0 2	46.403	1.955(7)	1.348	46.244	1.962(5)[b]	1.711	1.929	1.937
	46.639	1.946(4)	0.881	46.470	1.953(3)	1.244		
	46.775	1.941(5)	0.622	46.602	1.947(3)	0.933		
	46.869	1.937(2)	0.415	46.710	1.943(9)	0.726		
	46.930	1.935(5)	0.311					
	47.113	1.927(7)[b]	−0.104					
	47.440	1.915(9)	−0.725					
3 1 −2	62.866	1.477(11)	−0.337	63.637	1.461(2)	−1.417	1.482	1.486
	63.132	1.472(6)[b]	−0.675	63.735	1.459(1)[b]	−1.552		
	63.386	1.466(6)	−1.080					
	63.667	1.460(4)	−1.484					
	63.737	1.459(1)	−1.552					
1 −5 0	62.908	1.476(12)	0.408	63.681	1.460(2)	−0.680	1.470	1.452
	63.131	1.472(5)[b]	0.136	63.739	1.459(1)[b]	−0.748		
	63.342	1.467(4)	−0.204					
	63.571	1.462(7)	−0.544					
	63.724	1.459(1)	−0.748					

[a]Bulk parameters from Ref. 14.
[b]Dominant peak.

pair of very narrow lines (Table I) occurs at a high angle (lower d spacing) relative to the broad line profile found in the 2000-Å film (solid line) at a lower angle (higher d spacing). The high angle peaks in the thick film approximately match the peaks in the thin film.

In the 500-Å film the in-plane (3 1 −2) and (1 −5 0) reflections both yield dominant spacings of 1.459 Å and minor components with d spacings of ~1.460 Å. The corresponding values for the bulk are 1.482 and 1.470 Å, respectively, for the two reflections. We find that both in-plane directions are contracted relative to the bulk as expected for a film on a substrate of smaller lattice parameter ($a_p = 3.845$ Å in the bulk at 297 K vs $a_p = 3.791$ Å for the substrate). Note, however the existence of the secondary component with d spacing that is larger than the dominant peak. This suggests that there is a thin and more relaxed region of the film above the most heavily strained region relative to the substrate. We point out that the widths of the peaks are quite small for the in-plane dominant peaks of the 500-Å film indicating that the substrate has imposed its high structural order on the in-plane parameters of the film near the substrate-film interface.

In the thick film, the (3 1 −2) and (1 −5 0) reflections are represented by a broad distribution of peaks (see Table I). The d spacings vary from highly strained values found in the thin film to highly relaxed values approaching those found in bulk. However, the dominant layer of the film has an in-plane d spacing of 1.472 Å for both reflections compared to 1.482 and 1.470 Å found in the bulk. Hence in both the thin and thick films the substrate forces the films to be symmetric in plane. In other words, the in-plane constraint imposed by the substrate is not relieved in films up to 2000-Å thick.
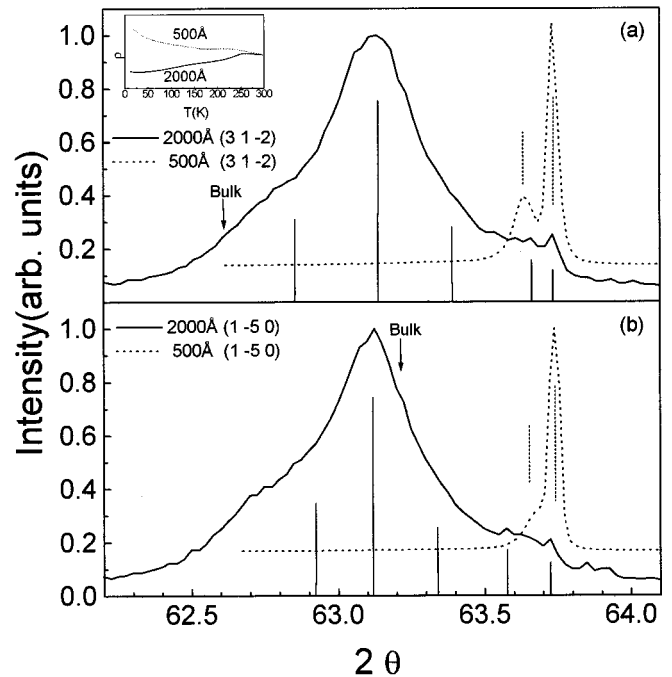

FIG. 1. X-ray-diffraction θ-2θ scans of $Nd_{0.5}Sr_{0.5}MnO_3$ film with the scattering plane approximately parallel to the surface. Diffraction peaks for (a) measurements along the direction (3 1 −2) and (b) along the direction (1 −5 0) are shown. The solid line is from the 2000-Å film and the dotted line is from the 500-Å film. Each pattern is fit by a set of Gaussian peaks and the vertical bars show the approximate peak positions. The position of the bulk diffraction lines is indicated by an arrow. The inset displays the resistivity data for the films.
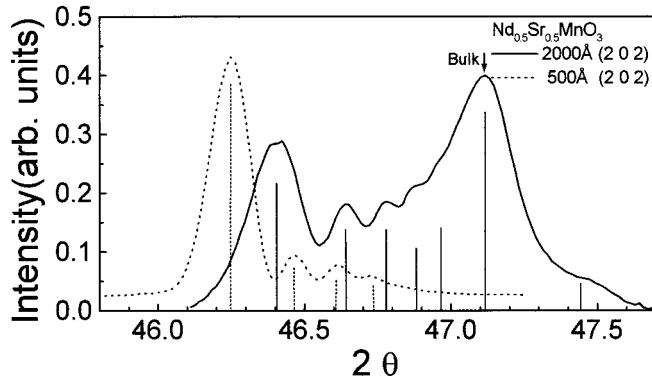
FIG. 2. X-ray-diffraction θ-2θ scans of $Nd_{0.5}Sr_{0.5}MnO_3$ films with the scattering plane normal to the surface and corresponding to the direction (2 0 2). The solid line is for the 2000-Å film and the dotted line is for the 500-Å film. Fits were performed as given in Fig. 1. The position of the bulk diffraction lines is indicated by an arrow.

Figure 2 shows the θ-2θ diffraction scan of 500- (dashed line) and 2000-Å (solid line) thick $Nd_{0.5}Sr_{0.5}MnO_3$ films for out-of-plane diffraction (sampling out-of-plane lattice spacings and along one set of Mn-O bonds). The dominant peak in the 500-Å film is observed at 46.24°, which corresponds to the out-of-plane (2 0 2) reflection and yields a layer spacing $d_{202} = 1.962$ Å (see Table I). In addition to this main peak, there is a series of smaller peaks at higher angles corresponding to the d parameters of 1.953, 1.947, and 1.943 Å. Consequently, the bulk of the film is in one strained region and a series of layers of reduced strain is found. On the other hand in the 2000-Å thick film, two dominant peaks are found yielding d spacings of 1.955 and 1.927 Å. A series of smaller peaks occur between these two dominant peaks. Note that the peak positions (see vertical lines) of the lines of the thick sample do not coincide with those of the thin sample.

The thin film is dominated by a layer near the substrate with $d = 1.962$ Å that is expanded relative to the bulk value of 1.929 Å as expected since the in-plane lattice parameters have contracted. A series of peaks with shorter lattice parameters are also found, supporting our model of discrete layer relaxation of strain.

In the thick film two dominant peaks occur. The main peak occurs at 1.927 Å (close to the bulk value of 1.929 Å) and the next dominant peak occurs at 1.955 Å. The thin layer near the substrate is forced to expand due to in-plane compression. Again, we see that, in addition to the dominant peaks, a set of peaks corresponding to intermediate relaxation is found in both films.

In Table I we also report the effective strain $\varepsilon_{hkl} = [d_{hkl}(\text{film}) - d_{hkl}(\text{bulk})]/d_{hkl}(\text{bulk})$ along the film normal (202) and near parallel directions to the film plane (3 1 -2) and (1 -5 0). These values should be compared to the expected strain value of -1.404% for $Nd_{0.5}Sr_{0.5}MnO_3$ (average $a = 3.845$ Å) on an $LaAlO_3$ substrate ($a = 3.791$ Å). In the thin film there is a large asymmetry between the strain found for the two in-plane directions—one direction is fully strained while the other is partially relaxed. In the thick films, the covering layers are less strained (in plane) but the asymmetry persists.
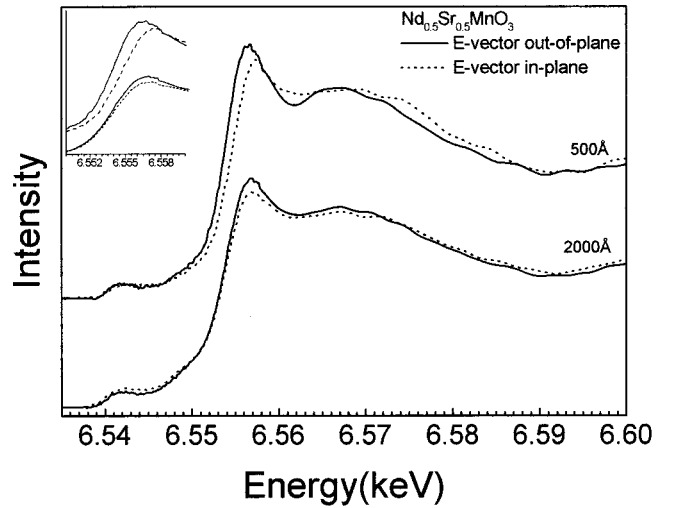

FIG. 3. Near-edge x-ray-absorption spectra (Mn K) of $Nd_{0.5}Sr_{0.5}MnO_3$ for 500- and 2000-Å films in fluorescent mode. The solid line is the spectrum measured when the incidence x-ray E vector is perpendicular to the film surface, while the dotted line is for the measurement with the incidence x-ray E vector parallel to the film surface. Inset shows the main edges in small range. Notice the asymmetry in the thin-film measurement suggesting local structural distortions.

For the thick film, the origin of this peak at 47.44° is not clear but may be due to a thin upper layer of the films contracting (below the bulk value) out of plane. Note the same region of the film may produce the expanded lattice parameter (beyond bulk) found in the (1 -5 0) in-plane peak at 62.908° [Fig. 1(b)]. A comprehensive thickness-dependent study of these films is in progress.

In order to correlate the changes in the long-range structure (found in XRD measurements) with changes in the local structure about the average Mn site, we measured polarized Mn K-edge absorption spectra of both films (Fig. 3), for directions in plane and out of plane. The inflection points in the spectra of the 500-Å film are separated by 0.7 eV compared to a separation of 0.0 eV for the thick film. We found that the edge position for the out-of-plane spectrum in the 500-Å film was the same as that found in the thick film for both orientations while the 500-Å in-plane spectrum shifted to higher energy.

Local structural information can be gleaned from polarized x-ray-absorption measurements. The main line corresponds to a $1s$ to $4p$ transition on the Mn site. In octahedral symmetry (at the Mn site) there is no orientational dependence of the Mn main line. In reduced symmetry, the $4p$ peak will split into two or three components with a progressive reduction in symmetry. Local distortions such as JT distortions produce such reductions in symmetry and generate orientational dependent splittings of the main line. In $LaMnO_3$ and other JT systems, broad main lines and splitting have been predicted and measured.[17,18] Consequently, the splitting seen in the $4p$ main line (Fig. 3) of the thin films is attributed to the existence of local distortions. In addition, models of polarized spectra indicate that measured spectra with lower edge positions correspond to the long bond direction.[17] Hence, for the thin strained film, the e_g orbitals

point preferentially out of plane. Interestingly, it is in the thin highly strained films with high in-plane order in which we find significant local distortions and orbital ordering.

Based on our chemical analysis the only difference between the two films is the degree of strain present. The pattern observed is that thin ($\sim$500-Å) $Nd_{0.5}Sr_{0.5}MnO_3$ films as well as bulk materials are highly insulating. Films of intermediate thicknesses show metallic behavior. This suggests that in this system there is an optimal strain value that will produce materials with high metallic properties. In the thin films, the strain induces JT distortions that stabilize the charge-ordered phase. In fact, even films that are metallic in bulk form display highly insulating behavior as thin films.[3,4,19] Our results suggest that the stabilization of JT distortions and possibly associated charge ordering occurs in highly strained manganites as a general rule.

We now return to the question concerning the origin of the insulator or metallic states of $Nd_{0.5}Sr_{0.5}MnO_3$ films. As seen in the inset of Fig. 1, thin films (less than 500 Å) are insulating while thick films ($\sim$2000 Å) are metallic. The analysis has shown that the thin films are severely strained with strain values characteristic of the lattice mismatch. In the thick films, while the out-of-plane strain contributes to a small volume of the films, the in-plane strain persists. We note also that the bulk materials, like neither of the films, displays an insulator-to-metal transition near 270 K that is overwhelmed by a metal-to-insulator transition concomitant with the onset of charge ordering at 150 K.[14]

The substrate-induced strain in the thin-film stabilized JT distortions as observed in the x-ray-absorption spectra. The trapping of the e_g electrons by these local distortions leads to the enhanced resistivity. In the thick film, on the other hand, the in-plane strain constrains the lattice parameters of the film and prevents the first-order transition to a charge-ordered phase that occurs in bulk materials.

High-resolution temperature-dependent measurements of the in-plane and out-of-plane lattice spacings across the bulk transition temperature to search for bulklike components will be carried out. In addition, further work is needed to specify the electronic structure of the thin films. The direct comparison of our results (on these films) with resonant x-ray scattering measurements[20] of orbital ordering will be instructive. Also, the asymmetry in strain suggests anisotropic in-plane transport. Hence, transport studies with different current directions will be carried out as a function of film thickness. The results will shed light on the magnetic asymmetries also seen in the films.

[1] Y. Tokura and Y. Tomioka, J. Magn. Magn. Mater. **200**, 1 (1999), and references therein; J. M. Coey, M. Verit, and S. von Molenar, Adv. Phys. **48**, 167 (1999), and references therein.

[2] S. Jin, T. H. Tiefel, M. McCormack, H. M. O'Bryan, L. H. Chen, R. Ramesh, and D. Schurig, Appl. Phys. Lett. **67**, 557 (1995).

[3] M. G. Blamire, B.-S. Teo, J. H. Durrell, N. D. Mathur, Z. H. Barber, J. L. McManus Driscoll, L. F. Cohen, and J. E. Evetts, J. Magn. Magn. Mater. **191**, 359 (1999).

[4] J. Z. Sun, D. W. Abraham, R. A. Rao, and C. B. Eom, Appl. Phys. Lett. **74**, 3017 (1999).

[5] Y. Suzuki, H. Y. Hwang, S.-W. Cheong, and R. B. van Dover, Appl. Phys. Lett. **71**, 140 (1997).

[6] X. W. Wu, M. S. Rzchowski, H. S. Wang, and Qi Li, Phys. Rev. B **61**, 501 (2000).

[7] H. S. Wang, Qi Li, Kai Liu, and C. L. Chien, Appl. Phys. Lett. **74**, 2212 (1999); H. S. Wang and Qi Li, *ibid.* **73**, 2360 (1998).

[8] T. K. Nath, R. A. Rao, D. Lavric, C. B. Eom, L. Wu, and F. Tsui, Appl. Phys. Lett. **74**, 1615 (1999).

[9] J. O'Donnell, M. S. Rzchowski, J. N. Eckstein, and I. Bozovic, Appl. Phys. Lett. **72**, 1775 (1998).

[10] A. J. Millis, T. Darling, and A. Migliori, J. Appl. Phys. **83**, 1588 (1998).

[11] A. J. Millis *et al.* (unpublished).

[12] Z. Fang, I. V. Solovyev, and K. Terakura, Phys. Rev. Lett. **84**, 3169 (2000).

[13] W. Prellier, A. Biswas, M. Rajeswari, T. Venkatesan, and R. L. Greene, Appl. Phys. Lett. **75**, 397 (1999).

[14] H. Kawano, R. Kajimoto, H. Yoshizawa, Y. Tomioka, H. Kuwahara, and Y. Tokura, Phys. Rev. Lett. **78**, 4253 (1997); H. Kuwahara, Y. Tomioka, A. Asamitsu, Y. Moritomo, and Y. Tokura, Science **270**, 961 (1995).

[15] H. L. Ju, C. Kwon, Q. Li, R. L. Greene, and T. Venkatesan, Appl. Phys. Lett. **65**, 2108 (1994).

[16] T. A. Tyson, Q. Qian, C-C. Kao, J.-P. Rueff, F. M. F. de Groot, M. Croft, S.-W. Cheong, M. Greenblatt, and M. A. Subramanian, Phys. Rev. B **60**, 4665 (1999).

[17] M. Benfatto, Y. Joly, and C. R. Natoli, Phys. Rev. Lett. **83**, 636 (1999).

[18] Q. Qian, T. A. Tyson, C.-C. Kao, M. Croft, S-W. Cheong, G. Popov, and M. Greenblatt (unpublished).

[19] Y. Konisha, Z. Fang, M. Izumi, T. Manako, M. Kasi, H. Kuwahara, M. Kawasaki, K. Terakura, and Y. Tokura, J. Phys. Soc. Jpn. **68**, 3790 (1999).

[20] M. v. Zimmermann, J. P. Hill, Doon Gibbs, M. Blume, D. Casa, B. Keimer, Y. Murakami, Y. Tomioka, and Y. Tokura, Phys. Rev. Lett. **83**, 4872 (1999); Y. Murakami, J. P. Hill, D. Gibbs, M. Blume, I. Koyama, M. Tanaka, H. Kawata, T. Arima, Y. Tokura, K. Hirota, and Y. Endoh, *ibid.* **81**, 582 (1998).